Effect of carbon nanotubes reinforcement on the mechanical properties of alumina and ZTA composites for ballistic application

(Efeito de reforço de nanotubos de carbono nas propriedades mecânicas de compósitos de alumina e ZTA para aplicação balística)

C. A. de O. Couto[1]*, S. Ribeiro[2], F. R. Passador[1]

[1]Federal University of São Paulo, Department of Science and Technology, R. Talim 330, 12231-280, São José dos Campos, SP, Brazil

[2]University of São Paulo, Department of Materials Engineering, Lorena, SP, Brazil

Abstract

Toughened and hardened alumina/carbon nanotubes and zirconia-toughened alumina (ZTA)/carbon nanotubes nanocomposites were developed by conventional ceramics route using pressureless sintering for the ballistic application. The multiwall carbon nanotubes (CNT) were functionalized with nitric acid oxidation reaction. Moreover, the surfactants sodium dodecyl sulphate and gum arabic were used to promote a homogeneous distribution of CNT in the ceramic matrix. Ceramic powders were prepared with pure alumina, alumina with the addition of 20 wt% of tetragonal zirconia/yttria, alumina/CNT and ZTA/CNT with the addition of 0.1 and 0.5 wt% of CNT. The morphology of nanocomposites was characterized by SEM-FEG. The mechanical properties of sintered samples were evaluated by flexural bending, Vickers microhardness and fracture toughness by SEVNB method. The addition of CNT in the ceramic and composite caused a general increase in densification, hardness, flexural strength and fracture toughness. ZTA composite with the addition of 0.1 wt% of CNT yielded the best results.

Keywords: alumina, zirconia, carbon nanotubes, nanocomposites.

Resumo

Nanocompósitos de alumina/nanotubos de carbono e alumina tenacificada com zircônia (ZTA)/nanotubos de carbono foram desenvolvidos por rota cerâmica convencional utilizando sinterização sem pressão para aplicação balística. Os nanotubos de carbono de parede múltipla (NTC) foram funcionalizados por reação de oxidação com ácido nítrico. Além disso, os surfactantes dodecil sulfato de sódio e goma arábica foram utilizados para promover uma distribuição homogênea de NTC na matriz cerâmica. Os pós cerâmicos foram preparados com alumina pura, alumina com adição de 20% em massa de zircônia tetragonal/ítria, alumina/NTC e ZTA/NTC com adição de 0,1 e 0,5% em massa de NTC. A morfologia dos nanocompósitos foi caracterizada por MEV-FEG. As propriedades mecânicas das amostras sinterizadas foram avaliadas por ensaio de flexão, microdureza Vickers e tenacidade à fratura pelo método SEVNB. A adição de NTC na cerâmica e no compósito causou aumento geral na densificação, dureza, resistência à flexão e tenacidade à fratura. O compósito ZTA com adição de 0,1% de NTC obteve os melhores resultados.

***Palavras-chave**: alumina, zircônia, nanotubos de carbono, nanocompósitos.*

INTRODUCTION

The ceramic armor is a tough and hard protection capable of fragmenting the projectile and reducing its speed during the impact, turning it into small fragments that are absorbed by the flexible bottom plate that supports the ceramic material. For this, it is necessary that the ceramic material has high mechanical resistance to deformation combined with high hardness. Fracture toughness, the property of a material to resist brittle fracture, is an important requirement for ballistic application [1]. Alumina (Al_2O_3) is the most used material to produce armor and presents an excellent cost-benefit ratio among advanced ceramics. Alumina presents a high modulus of elasticity, high refractoriness, high hardness, and commercial viability. However, it has low fracture toughness, low flexural strength and also low electrical and thermal conductivity that restrict the use of this material. Additives that modify the mechanical and functional properties of the alumina matrix, for example, zirconia, are used to improve the limitations of monolithic alumina and increase its performance [2, 3]. Zirconia may be added to the alumina matrix to improve its toughness by a homogeneous distribution of the zirconia phase. It is possible to inhibit the grain growth of the alumina phase during the sintering process. Several investigations showed that a smaller grain size in alumina ceramics leads to better wear resistance and mechanical properties [4-6]. The zirconia exists in three polymorphic crystalline structures:

**carlos.couto.sjc@gmail.com*

monoclinic, tetragonal and cubic. Monolithic zirconium oxide has a monoclinic structure at room temperature and this phase is stable up to 1170 °C. Above this temperature, it becomes tetragonal and then cubic at 2370 °C. Tetragonal zirconia stabilized with 3 mol% of yttria (3Y-TZP) is used in many structural applications due to its excellent mechanical properties, which are related to the stress shielding effect by toughening transformation and the formation of sub-micrometric grain size. Tetragonal to monoclinic (T→M) phase transformation plays a key role in avoiding the crack extension from external stresses as the zirconia grain expands, closing the crack. T→M transformation is analogous to the martensitic transformation. Expansion from 3 to 5% in volume and the shear strain developed during this transformation result in a compressive deformation in the matrix. These phenomena restrict crack propagation. For crack propagation, an additional energy is required, thus increasing the fracture toughness and tensile strength [7, 8].

The carbon nanotubes (CNT) have excellent mechanical properties, high elastic modulus and chemical inertia. Furthermore, the carbon nanotubes are self-lubricating, which facilitates the ceramic composites compression process. The use of multi-wall carbon nanotubes (MWCNT) or single-wall carbon nanotubes (SWCNT) as filler in ceramic matrices produce composites with better mechanical properties, such as fracture toughness, flexural strength and Young's modulus. This improvement is mainly due to two mechanisms: the bridging and the pull-out effects on the fracture surfaces when the crack is subjected to a tensile load [9, 10]. During the sintering of alumina in the presence of carbon nanotubes carbothermal reduction can occur and, depending on the temperature and pressure of the system, it may form Al_2OC, Al_4O_4C or Al_4C_3. In low-pressure systems using temperature between 1500 and 1700 °C, the formation of Al_2OC and Al_4O_4C occurs preferentially due to the similarity of size with Al_2O_3. Temperatures above 1700 °C facilitate the formation of Al_4C_3 that damages the structure of the nanocomposites. The interface between Al_2OC/Al_4O_4C and alumina/CNT is chemically compatible and favors the production of Al_2O_3/CNT structural nanocomposites [11]. A better understanding of the thermomechanical behavior of carbon nanotube nanocomposites requires knowledge of the elastic and fracture properties of CNT as well as the interface interaction between the reinforcement and the matrix [12]. Another challenge for increasing the mechanical properties of the nanocomposites is to avoid the aggregation of carbon nanotubes during processing; this undesired occurrence is due to the chemical inertness of CNT caused by their unique sp^2 bonding in the graphene layers and their complex entanglement due to strong van der Waals forces. Such entangled bundles of carbon nanotubes cause a significant reduction on the mechanical properties of nanocomposites. The effective use of carbon nanotubes in composite applications strongly depends on the ability to homogeneously disperse and distribute the reinforcement throughout the matrix. However, CNT high aspect ratio and small diameter contribute to a poor dispersion. Furthermore, a good interfacial bonding is required to have a load transfer across the interface from the ceramic matrix to the CNT, resulting in an effective application of the reinforcement [13]. Microstructural observations have shown that CNT can be homogeneously mixed in the matrix at a microscopic level with the addition of low content of CNT. However, when CNT content is increased by over 2.0 wt% the formation of bundles occurs [14, 15]. A study [16] concluded that the ceramic microstructure is the main factor affecting ballistic performance. Accordingly, some studies have investigated the influence of inclusions, grain size and grain size variation as well as porosity in the ceramic matrix [17]. The microstructure is known to control the performance of ceramics during ballistic events through crack propagation and energy dissipation mechanisms [18]. A uniform microstructure with little porosity is the most desirable, although a small percentage of well-distributed porosity may still guarantee high ballistic resistance [17].

In order to promote a good dispersion of CNT in alumina and ZTA matrix, polyethylene glycol (PEG), gum arabic (GA) and sodium dodecyl sulphate (SDS) were used. Gum arabic and sodium dodecyl sulphate are effective water-soluble dispersants, which can promote the dispersion of CNT by electrostatic and steric repulsions. CNT coated with GA and SDS was negatively charged. PEG mixed in the matrix turned the ceramic particles positively charged promoting interfacial bonding [19-22]. The focus of this study was to investigate the effect of adding 0.1 and 0.5 wt% of CNT on the mechanical properties of alumina and ZTA composite. The results were compared and correlated with the pure ceramics.

EXPERIMENTAL

Materials: the micronized alumina (Al_2O_3) commercially designated as APC-G was supplied by Alcoa (Brazil). The micro and nanoparticulated tetragonal zirconia stabilized with 3 mol% of yttria (3Y-TZP) was supplied by Zhongshun (China). The multi-wall carbon nanotubes (CNT) with 95% purity, diameter less than 8 nm and length of 10-30 μm were supplied by Nanostructured and Amorphous Materials (USA). Gum arabic (GA, 51200) was supplied by Fluka, and sodium dodecyl sulphate (SDS, L6206) and polyethylene glycol (PEG, 202436) were supplied by Sigma-Aldrich.

Functionalization of CNT: the surfaces of CNT were functionalized with carboxyl groups by oxidation reactions with nitric acid. For the oxidation reaction, 4 g of CNT was added to 500 mL of HNO_3 solution at 3 $mol.L^{-1}$. This solution was refluxed for a period of 12 h at 120 °C. After the oxidation period, the solution was centrifuged for 20 min at 20 ºC and 4500 rpm, washed with distilled water, followed by vacuum filtration.

Preparation and sintering of Al_2O_3, ZTA composite, Al_2O_3/CNT and ZTA/CNT nanocomposites. Ceramic and composite: ZTA composite (Al_2O_3 with 20 wt% of ZrO_2) with 1 wt% of diluted PEG and distilled water was prepared using a ball mill for 14 h in a polyethylene jar. The mixture was

dried at 100 °C for 24 h and ground and sieved using a 200 mesh sieve. Green samples (4 x 5 x 40 mm^3) were prepared by uniaxial pressing at 60 MPa with a steel mold, followed by cold isostatic pressing at 300 MPa. Samples were finally pressureless sintered at 1450, 1500, 1550 and 1600 °C for 2 h using a heating rate of 10 °C.min^{-1} with argon atmosphere in a high temperature oven (Thermal Technology, 1000-4560-FP20). Pure Al_2O_3 with 1 wt% of diluted PEG were also prepared using the same method. *Nanocomposites*: for Al_2O_3/CNT and ZTA/CNT nanocomposite preparations, CNT/SDS/GA (50/35/15 wt%) and surfactants were hand-mixed for 2 min in ethanol solution to negatively charge the carbon nanotubes. Then, the suspension was dispersed for 10 min using an ultrasonic processor (Sonics Vibra Cell, VCX 750) at 30% of the equipment intensity. Alumina and zirconia powders (80/20 wt%) were mixed with a diluted PEG (1 wt%) distilled water solution for 30 min to make the powders positively charged. Then, CNT/SDS/GA dispersed suspensions containing 0.1 and 0.5 wt% of CNT were mixed with alumina/PEG suspensions in a ball mill for 14 h. Forming and sintering conditions were the same as for ZTA composites. Table I shows the compositions studied in this work.

Table I - Compositions studied.
[Tabela I - Composições estudadas.]

Identification	Composition
1	Al_2O_3 + 0.5 wt% CNT
2	Al_2O_3 + 0.1 wt% CNT
3	ZTA + 0.5 wt% CNT
4	ZTA + 0.1 wt% CNT
5	Pure Al_2O_3
6	Pure ZTA

Characterization of the ceramics and nanocomposites: the samples (3.2 x 4.2 x 32 mm^3) were tested using a three-point bending device in an Instron machine (mod. 430) to obtain the flexural strength. The fracture toughness was evaluated using the single-edge V-notched beam (SEVNB) method according to ISO 23146:2008. Microstructural analyses were performed on the tested samples by scanning electron microscopy (SEM-FEG) and X-ray diffraction (XRD). Fractured surfaces were covered with a thin layer of gold and were observed in an FE-SEM Mira3, Tescan, operating at 15 kV. The composite phases were analyzed using an X-ray diffractometer (Rigaku, Ultima IV) operated at 0.2 °.s^{-1} and 2θ ranging from 10° to 90°. In order to measure the grain size of the samples, the surfaces were polished and etched with H_3PO_4 (85%) for 10 min at 250 ºC [23]. The prepared surfaces were observed in an SEM (FEI, Inspect S50). The samples' micrographs were analyzed using Image-J software to obtain the grain size (D_{50}). The microhardness of the samples was measured with a microhardness tester (Future-tech, FM-7). The density of the sintered samples was evaluated by Archimedes water immersion technique. Theoretical density and densification of the nanocomposites were calculated using the rule of mixture, considering values of 3.96 g.cm^{-3} for alumina density and 6.04 g.cm^{-3} for tetragonal zirconia density (according to supplier specification). ZTA's calculated density was 4.376 g.cm^{-3}. The porosity of samples was evaluated by the nitrogen adsorption technique. The adsorption and desorption curves were obtained with a Quantachrome Nova (4200e) with the samples' pretreatment at 300 °C for 4 h in vacuum to remove impurities from the surface.

RESULTS AND DISCUSSION

Fig. 1 shows the densification of the compositions 1 to 6 sintered at 1450 to 1600 °C under argon atmosphere. Pure ZTA samples (composition 6) presented low densification for the selected temperatures compared with nanocomposite 4 (ZTA+0.1 wt% CNT), which achieved a densification of 99.2% sintered at 1600 °C. Pure alumina and alumina/CNT obtained similar densification. The complete densification was prevented by the size of the ceramic particles which was coarse. The carbon nanotubes possibly acted as solid lubricants, improving the ZTA particle packing. The mechanical tests were only performed for the samples sintered at 1500 and 1600 °C. The selection of these temperatures was according to the densification results. In addition, it was expected to obtain a smaller grain size at 1500 ºC than at 1600 ºC, so the correlation between sintering temperature, grain size, porosity and mechanical properties could be evaluated. The alumina particle size (D_{50}) was 0.35 μm and the surface area was 6.0 $m^2.g^{-1}$. For the zirconia powder, it was not possible to obtain primary particle size because the nanoparticles were agglomerated; its surface area was 42 $m^2.g^{-1}$ and mean pore diameter was 6.6 nm. Fig. 2 shows the XRD patterns of nanocomposites. Fig. 2a shows the results of compositions 1 (Al_2O_3+0.5 wt% CNT) and 2 (Al_2O_3+0.1 wt% CNT); only the α-alumina phase was observed for both compositions. Fig. 2b shows

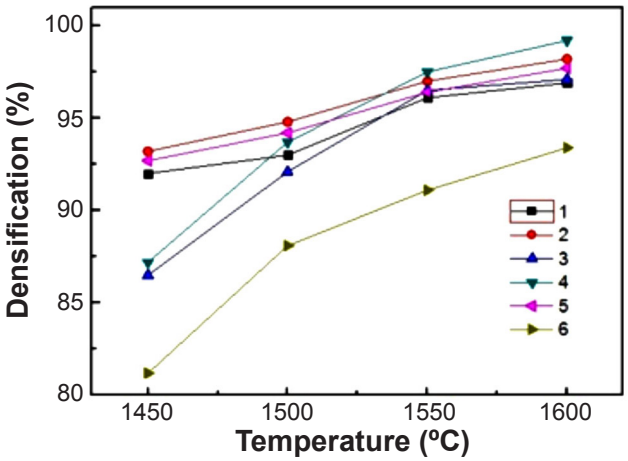

Figure 1: Densification of samples of compositions 1 to 6 sintered at different temperatures.
[Figura 1: Densificação das amostras de composições 1 a 6 sinterizadas em diferentes temperaturas.]

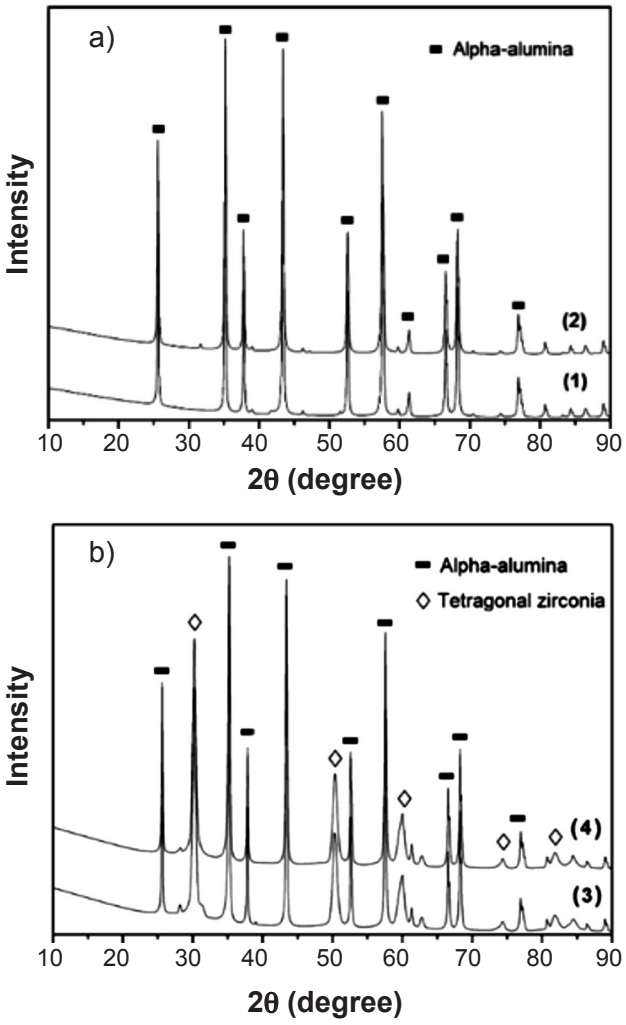

Figure 2: X-ray diffraction patterns of nanocomposites 1 and 2 (a), and 3 and 4 (b).
[Figura 2: Difratogramas de raios X dos nanocompósitos 1 e 2 (a) e 3 e 4 (b).]

the XRD patterns of compositions 3 (ZTA+0.5 wt% CNT) and 4 (ZTA+0.1 wt% CNT); the alumina was found as α-alumina phase and the zirconia as tetragonal phase, for both compositions.

Fig. 3a shows the grain size (D_{50}) and Fig. 3b shows the porosity of the ceramics and nanocomposites sintered at 1500 and 1600 °C. Carbon nanotubes limited the grain growth in alumina and ZTA composite. Nanocomposites with 0.1 wt% of CNT in most cases had larger grain sizes than 0.5 wt% of CNT nanocomposites. The nanocomposite 3 (ZTA+0.5 wt% CNT) sintered at 1500 ºC presented the smallest grains compared to all samples. However, at 1600 ºC, nanocomposite 4 (ZTA+0.1 wt% CNT) had the smallest grain size for this sintering temperature. It is possible that the zirconia particles also contributed to the grain growth control for ZTA composites. Studies show that smaller grains contribute to better ballistic efficiency along with other physical properties. Holland and McMeeking [24] positively correlated the high fracture strength and low porosity of the ceramic for a good ballistic performance

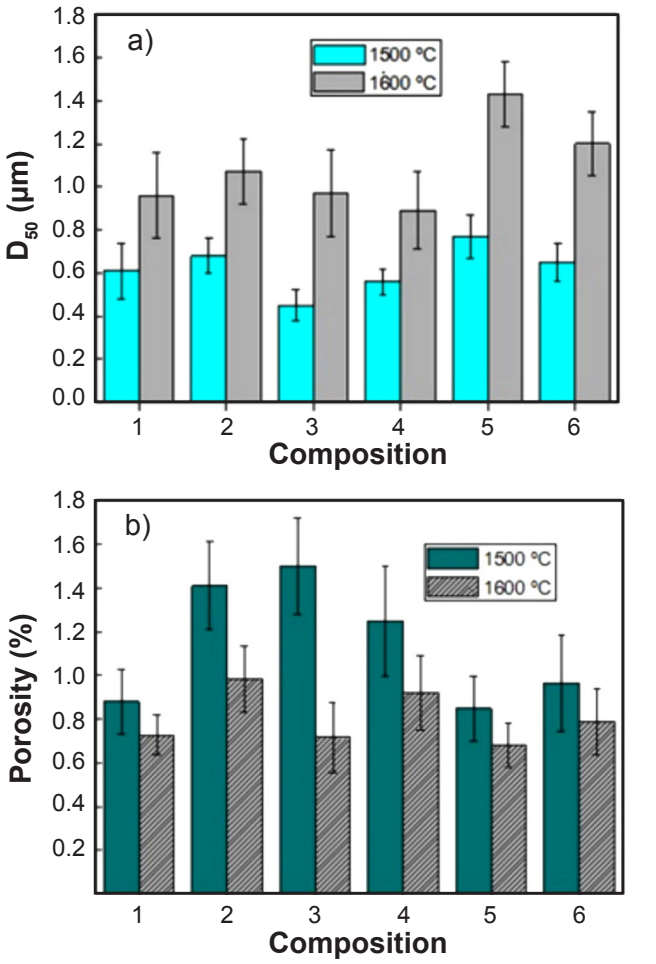

Figure 3: Grain size, D_{50} (a), and porosity (b) of compositions 1 to 6.
[Figura 3: Tamanho de grão, D_{50} (a), e porosidade (b) das composições 1 a 6.]

of the ceramic. Fig. 3b shows that nanocomposites with 0.5 wt% of CNT sintered at 1600 ºC presented the lowest porosity. The main challenge in ceramic processing is to obtain a microstructure that offers the best combination of properties. The variables that control the microstructure of ceramics are the initial raw material (particle size, shape and purity), forming process, powder sintering, final grain size, contraction, porosity, additives and densification method. It is important that all stages of production are controlled to obtain a homogeneous and refined microstructure [25, 26].

Table II shows the mechanical and physical properties for the compositions studied. Compositions sintered at 1600 ºC obtained higher flexural strength, fracture toughness and hardness compared to the same compositions sintered at 1500 ºC. There was an average increase of 12.9% in flexural strength, 3.7% in fracture toughness and 22.1% in hardness. Comparing the nanocomposites results with those of ceramics sintered at 1600 ºC: i) *nanocomposite 1* (Al_2O_3+0.5 wt% CNT) showed an improvement of 4.2% in flexural strength, 4.7% in fracture toughness and 9.7% in hardness compared to pure alumina (composition 5); ii) *nanocomposite 2* (Al_2O_3+0.1 wt% CNT) showed an improvement of 3.3% in flexural strength and

Table II - Mechanical and physical properties of the composites and nanocomposites.
[Tabela II - Propriedades mecânicas e físicas dos compósitos e nanocompósitos.]

Sample-sintering temperature	Flexural strength σ_f (MPa)	K_{Ic} (MPa.m$^{0.5}$)	Microhardness Hv (GPa)	ϱ (g.cm^{-3})	Relative density (%)
1-1500 °C	382 ± 23	4.1 ± 0.4	13.1 ± 1.4	3.68 ± 0.05	93.0 ± 1.3
2-1500 °C	369 ± 16	4.5 ± 0.4	12.1 ± 1.4	3.72 ± 0.06	94.8 ± 0.7
3-1500 °C	438 ± 21	4.8 ± 0.3	11.6 ± 0.6	4.03 ± 0.02	92.1 ± 0.5
4-1500 °C	466 ± 34	5.2 ± 0.5	11.8 ± 0.9	4.10 ± 0.02	93.7 ± 0.5
5-1500 °C	349 ± 36	3.9 ± 0.5	11.9 ± 0.7	3.75 ± 0.02	94.7 ± 0.5
6-1500 °C	334 ± 18	4.2 ± 0.2	10.5 ± 0.7	3.86 ± 0.05	88.1 ± 1.1
1-1600 °C	443 ± 46	4.4 ± 0.2	15.7 ± 0.6	3.84 ± 0.02	96.9 ± 0.5
2-1600 °C	439 ± 58	4.3 ± 0.2	15.2 ± 1.4	3.89 ± 0.03	98.2 ± 0.8
3-1600 °C	448 ± 44	5.1 ± 0.4	14.5 ± 1.5	4.25 ± 0.02	97.1 ± 0.5
4-1600 °C	481 ± 49	5.5 ± 0.4	14.6 ± 1.3	4.34 ± 0.03	99.2 ± 0.7
5-1600 °C	425 ± 58	4.2 ± 0.3	14.3 ± 0.6	3.87 ± 0.03	97.7 ± 0.7
6-1600 °C	403 ± 27	4.6 ± 0.2	12.4 ± 1.3	4.09 ± 0.04	93.4 ± 0.9

6.3% in hardness compared to pure alumina; Sarkar and Das [11] also obtained better results for alumina nanocomposite (pressureless sintered at 1600 ºC, containing 0.6 vol% CNT) compared to pure alumina; their best results were hardness of 21 GPa, SEVNB K_{Ic} of 4.4 MPa.m$^{0.5}$ and flexural strength of 265 MPa, which are compatible with the results of the present study; iii) *nanocomposite 3* (ZTA+0.5 wt% CNT) showed an improvement of 11.1% in flexural strength, 10.9% in fracture toughness and 16.9% in hardness compared to pure ZTA (composition 6); iv) *nanocomposite 4* (ZTA+0.1 wt% CNT) had an improvement of 19.3% in flexural strength, 19.6% in fracture toughness and 17.7% in hardness compared to pure ZTA (composition 6). Zhu *et al*. [3] studied ZrO_2 nanoparticles synthesized *in situ* on the surfaces of CNT and then applied to alumina ceramic to obtain good CNT dispersion in the ceramic matrix. ZTA nanocomposite with 1.5 wt% of CNT and 25 wt% of ZrO_2 resulted in flexural strength of 500 MPa, while in pure ZTA was 365 MPa; the fracture toughness values were 7.8 and 5.2 MPa.m$^{0.5}$, respectively, but the method used (JIS R1607-1995) was different from the SEVNB. The flexural strength of ZTA nanocomposite was similar to this study, but the processing of nanocomposite was simpler in the present study. The carbon nanotubes in the composites contributed to a general improvement in the mechanical properties, especially for the ZTA composite.

There is no clear correlation between the mechanical properties and ballistic behavior of the ceramic material during ballistic impact, due to complex stress mechanism involved in the impact. However, some parameters, such as hardness, fracture toughness, flexural strength and modulus of elasticity, have some degree of influence [27]. A high hardness of the ceramic is desirable, since the hardness influences the dwell time [28] and reduces the penetration of the projectile, since the material is capable of fragmenting a projectile during impact [29]. In addition, when the ceramic plate is fragmented by the projectile, the ceramic fragments of high hardness cause more abrasion of the projectile during the penetration process [30]. However, it is not clear whether a high hardness is always better, since the ductile failure mode is preferred for the ceramic plate in shielding solutions, and it is known that usually the higher the hardness the more brittle the material is. Preventing or delaying ceramic failure is crucial for its protection ability, so the ceramic must withstand the flexural stresses that occur during impact. In this sense, the fracture toughness, K_{Ic}, can give an indication of ceramic performance [31]. One of the most used empirical equations is the energy dissipation (D) criterion developed in [32], according to:

$$D = 0.36.Hv.E.c.K_{Ic}^{-1} \quad (A)$$

where Hv is the Vickers microhardness, E is the elastic modulus, c is the sound velocity and K_{Ic} is the fracture toughness. However, Eq. A suggests that the higher the fracture toughness the less energy is dissipated. This contrasts sharply with the general notion of improving ballistic performance of the ceramic plate by increasing its fracture toughness. This equation may be used for single shot and hard-core projectile. For multiple shots, a high fracture toughness is preferable [27], especially for the ductile-core projectile. Therefore, a simplified merit index for the ceramic plate is proposed for comparative evaluation among the various compositions developed in this work, considering the main properties for the ballistic application, and taking into account many related studies. Eq. B presents this merit index (MI):

$$MI = \sigma_f.K_{Ic}.Hv.\varrho^{-1} \quad (B)$$

where σ_f is the flexural strength, K_{Ic} is the fracture toughness, Hv is the Vickers microhardness and ϱ is the density (Table II). Fig. 4 shows the merit index values of the studied compositions sintered at 1500 and 1600 ºC. The

nanocomposite 4 (ZTA+0.1 wt% CNT) sintered at 1600 °C resulted in the highest merit index, 58% higher than the pure ZTA sintered at the same temperature. Although the nanocomposite 1 (alumina with 0.5 wt% CNT) did not result in a great improvement in the flexural strength and fracture toughness, the overall performance of this nanocomposite sintered at 1600 ºC was good, surpassing the nanocomposite 3, with a performance only 11% lower than the nanocomposite 4. Ballistic performance of a given material also depends on the type of ammunition used; projectiles may have different speed, hardness and mass. Ceramic hardness, one of the properties of the merit index, may have the most influence when the projectile is a perforating type, usually with WC hardened core. However, when a ceramic plate is subjected to multiple high-energy impacts, there is a need to maintain its structural integrity. In this case, the high fracture toughness is the most important property. Another important property is the flexural strength; Zhang and Li [31] demonstrated that not only the hardness but also the strength of the ceramic significantly affects the fragmentation process. In addition, their ballistic study of alumina and ZTA ceramics showed that the ballistic resistance of ZTA was higher than that of alumina due to increased K_{Ic} [31]. In addition, ZTA ceramics essentially exhibit a pattern of primary cracks accompanied by an intergranular failure mode. Previous studies have shown that the mode of intergranular failure of low porosity materials, such as ZTA ceramics, has a greater potential for energy absorption. Small grains favor intergranular failure with higher fracture toughness and large grains to transgranular failure with low fracture toughness [26]. The ZTA nanocomposites of the present study resulted in flexural strength and K_{Ic} values higher than alumina nanocomposites and much higher than pure alumina ceramic. The results of the merit index were in accordance with the results obtained by other researchers [7, 31], as the nanocomposite 4 (ZTA+0.1 wt% CNT) resulted in the highest merit index, at both sintering temperatures. Although the values obtained for the ballistic merit index are not absolute for performance evaluation of the ceramic composites, they help in a general evaluation of the material.

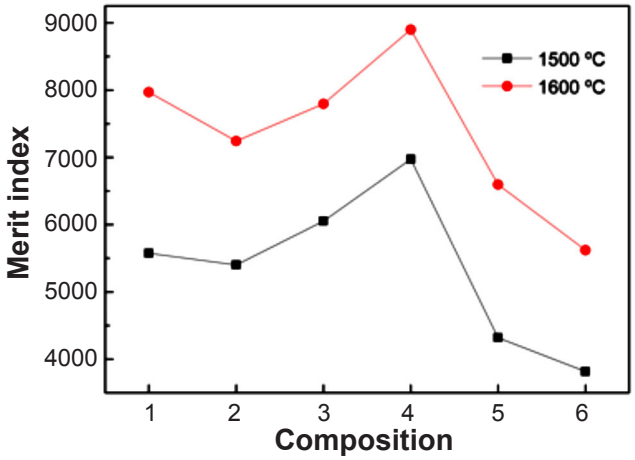

Figure 4: Merit index values of the studied compositions.
[Figura 4: Valores de índice de mérito das composições estudadas.]

Fig. 5A shows the micrographs of fractured surfaces obtained by SEM for nanocomposite 1 (alumina with addition of 0.5 wt% CNT) sintered at 1500 ºC (a) and 1600 ºC (b). The sample sintered at 1500 ºC presented good dispersion of carbon nanotubes but it was possible to observe the formation of nonhomogeneous morphology for both samples. The black arrows in the micrographs indicate the presence of CNT at the grain boundaries. Fig. 5B shows the micrographs of the composition 2 (Al_2O_3+0.1 wt% CNT) sintered at 1500 ºC (a) and 1600 ºC (b). The sample sintered at 1500 ºC presented many pores and low densification but it was possible to observe carbon nanotubes at the grain boundaries. It was also observed that the increase in temperature tended to favor the alumina carbothermal reduction. Fig. 5C shows

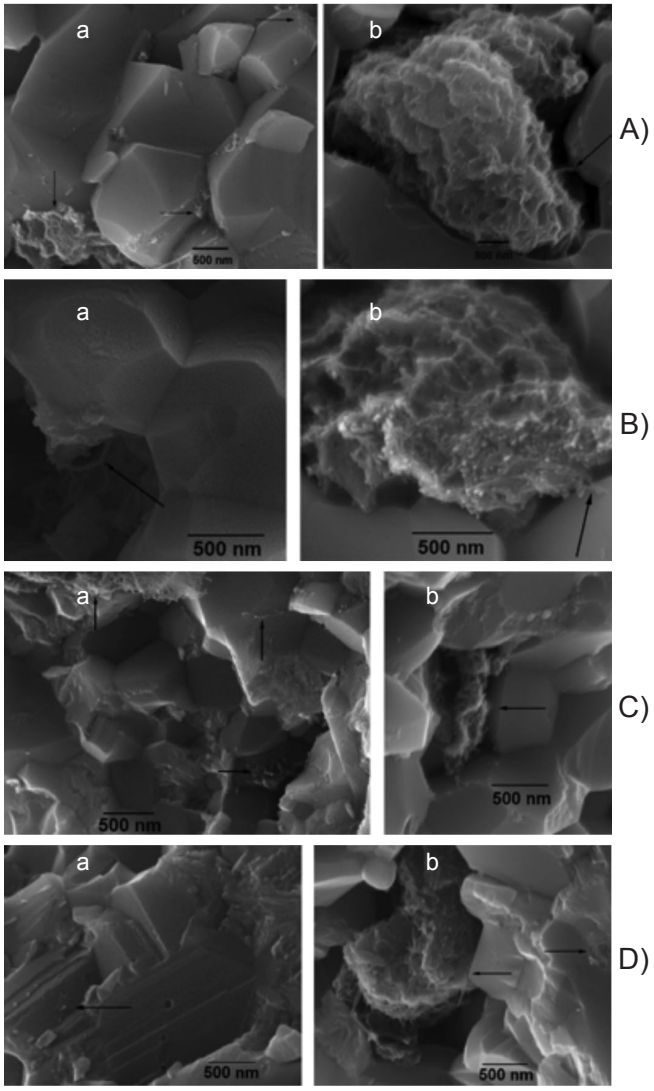

Figure 5: SEM micrographs of fractured surfaces of nanocomposites Al_2O_3+0.5 wt% CNT (A), Al_2O_3+0.1 wt% CNT (B), ZTA+0.5 wt% CNT (C), and ZTA+0.1 wt% CNT (D), sintered at 1500 ºC (a) and 1600 ºC (b).
[Figura 5: Micrografias de MEV das superfícies de fratura de nanocompósitos Al_2O_3+0,5% NTC (A), Al_2O_3+0,1% NTC (B), ZTA+0,5% NTC (C) e ZTA+0,1% NTC (D), % em massa, sinterizados a 1500 ºC (a) e 1600 ºC (b).

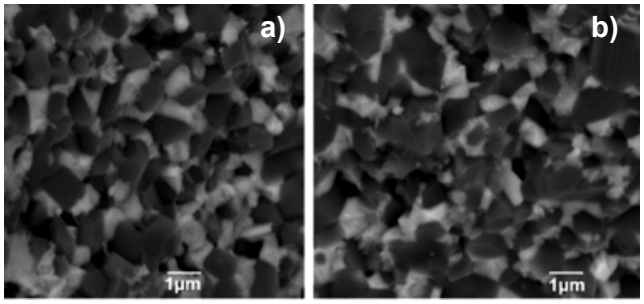

Figure 6: BSE images (SEM) of fractured surfaces of ZTA nanocomposites sintered at 1600 °C with: a) 0.5 wt% CNT; and b) 0.1 wt% CNT.
[Figura 6: Imagens de elétrons retroespalhados (MEV) das superfícies de fratura de nanocompósitos ZTA sinterizados a 1600 °C com: a) 0,5% em massa de NTC; e b) 0,1% em massa de NTC.]

the micrographs of the composition 3 (ZTA+0.5 wt% CNT). The addition of zirconia inhibited the grain growth and the microstructures presented isolated concentration of carbon nanotubes. Fig. 5D shows the morphology of the composition 4 (ZTA+0.1 wt% CNT) sintered at 1500 and 1600 ºC. The CNT in the samples were better distributed, compared to the samples in Fig. 5C. This good dispersion may explain the better results for mechanical properties of this nanocomposite.

Fig. 6 shows the fracture morphology of the compositions 3 and 4 sintered at 1600 ºC using BSE (backscattered electron) detector. The zirconia grains (small white grains) were homogeneously distributed in the alumina matrix. It was possible to observe a fine texture caused by the carbon nanotubes. It was also observed that the addition of a small amount of CNT had a considerable influence on the densification of ZTA nanocomposites, however, in alumina nanocomposites, this influence was lower. ZTA nanocomposites showed a better distribution of CNT and inhibited the alumina carbothermal reduction.

CONCLUSIONS

Carbon nanotubes significantly improved the mechanical properties of the ZTA and alumina nanocomposites; the nanotubes increased the densification and inhibited grain growth during the sintering process, and reinforced the matrix, increasing the fracture toughness, flexural strength and hardness. The ZTA/CNT nanocomposite (0.1 wt% CNT) sintered at 1600 °C achieved the highest mechanical properties (flexural strength and fracture toughness) and the smallest grain size among the tested nanocomposites. ZTA and alumina nanocomposites reinforced with CNT (0.1 or 0.5 wt%) manufactured through the conventional ceramic route proved to have a great potential for use in ballistic shielding application.

ACKNOWLEDGEMENTS

The authors would like to thank FAPESP (2014/04900-9) and CNPq for the financial support.

REFERENCES

[1] M.V. Silva, D. Stainer, H.A. Al-Qureshi, O.R.K. Montedo, D. Hotza, J. Ceram. **2014** (2014) 618154.
[2] M. Michálek, M. Kasiarová, M. Michálková, D. Galusek, J. Eur. Ceram. Soc. **34** (2014) 3329.
[3] Y.-F. Zhu, L. Shi, J. Liang, D. Hui, K.-T. Lau, Compos. B. Eng. **39** (2008) 1136.
[4] M.R. Falvo, G.J. Clary, R.M. Taylor II, V. Chi, F.P. Brooks Jr., S. Washburn, R. Superfine, Nature **389** (1997) 582.
[5] R.K. Chintapalli, F.G. Marro, B. Milson, M. Reece, M. Anglada, Mat. Sci. Eng. A **549** (2012) 50.
[6] D. Casellas, M.M. Nagl, L. Llanes, M. Anglada, J. Mater. Process. Technol. **143** (2003) 148.
[7] C. Piconi, G. Maccauro, Biomaterial **20** (1999) 1.
[8] S.P.S. Badwal, Solid State Ionics **52** (1992) 23.
[9] R.S. Lee, H.J. Kim, J.E. Fischer, A. Thess, R.E. Smalley, Nature **388** (1997) 255.
[10] P. Kim, L. Shi, A. Majumdar, P.L. McEuen, Phys. Rev. Lett. **87** (2001) 215502.
[11] S. Sarkar, P.K. Das, Ceram. Int. **38** (2012) 423.
[12] E.T. Thostensona, Z. Renb, T.-W. Chou, Compos. Sci. Technol. **6** (2001) 1899.
[13] F. Inam, H. Yan, D.D. Jayaseelan, T. Peijs, M.J. Reece, J. Eur. Ceram. Soc. **32** (2010) 153.
[14] G. Yamamoto, M. Omori, K. Yokomizo, T. Hashida, Diam. Relat. Mater. **17** (2008) 1554.
[15] C.B. Mo, S.I. Cha, K.T. Kim, K.H. Lee, S.H. Hong, Mat. Sci. Eng. A **395** (2005) 124.
[16] A. Krell, E. Strassburger, in: 27th Int. Symp. Ballistics (2013) 1053.
[17] M.P. Bakas, "Analysis of inclusion distributions in silicon carbide armor ceramics", Ph.D. Thesis (2006), State Un. New Jersey Rutgers.
[18] D.A. Shockey, J.W. Simons, D.R. Curran, Int. J. Appl. Ceram. Technol. **7**, 5 (2010) 566.
[19] F. Inam, A. Heaton, P. Brown, M.J. Reece, Ceram. Int. **40** (2014) 511.
[20] F Inam, H.X. Yan, T. Peijs, M.J. Reece, Compos. Sci. Technol. **70** (2010) 947.
[21] F. Inam, T. Peijs, J. Nanostruct. Polym. Nanocompos. **2** (2006) 87.
[22] O. Vasylkiv, Y. Sakka, V.V. Skorokhod, J. Am. Ceram. Soc. **86** (2003) 299.
[23] U. Taffner, V. Carle, U. Schafer, in: ASM Handb., vol. 9, ASM Int., Mater. Park (2004) 1057.
[24] C.C. Holland, R.M. McMeeking, Int. J. Impact Eng. **81** (2015) 34.
[25] G. Magnani, L. Beaulardi, L. Pillotti, J. Eur. Ceram. Soc. **25** (2005) 1619.
[26] D. Goncalves, F.C.L. De Melo, A. Klein, H.A. Al-Qureshi, Int. J. Mach. Tool Manuf. **44** (2004) 307.
[27] E. Medvedovski, Ceram. Int. **36** (2010) 2103.
[28] P. Lundberg, B. Lundberg, Int. J. Impact Eng. **31**, 7 (2005) 781.
[29] S.M. Walley, Adv. Appl. Ceram. **109**, 8 (2010) 446.

[30] J. La Salvia, J. Campbell, J. Swab, J. McCauley, JOM **62**, 1 (2010) 16.
[31] X. F. Zhang, Y.C. Li, Mater. Design **31** (2010) 1945.
[32] V.C. Nesphor, G.P. Zaitsav, E.J. Dovgal, A.L. Maystrenko, O.B. Dasevskaya, in: Proc. 8th CIMTEC, Italy (1995) 2395.
(Rec. 28/11/2017, Rev. 27/03/2018, 29/05/2018, Ac. 06/06/2018)